Biomimetics Biomaterials and Tissue Engineering

Menzies et al., J Biomim Biomater Tissue Eng 2013, 18:1
http://dx.doi.org/10.4172/1662-100X.1000105

Research Article Open Access

A Nested-Lumen Nerve Graft Design for Neuroengineering

Cameron H Menzies[1], Antonio Lauto[2], Lloyd Mirto[2], Ben Van Gogh[1], Andrew Ruys[1], Sri Bandyopadhyay[3], Paul Carter[4] and Philip Boughton[1]*

[1]*Biomedical Engineering, AMME School, The University of Sydney, Sydney, Australia*
[2]*Medical Science SoSH, University of Western Sydney, Sydney, Australia*
[3]*School of Materials Science & Engineering, University of New South Wales, Sydney, Australia*
[4]*Cochlear Pty Ltd, Sydney Australia*

Abstract

A biomimetic nerve graft design was developed for use in peripheral nerve regeneration. Nerve endings are difficult to suture or enjoin without support and autograft techniques also lead to added morbidity. Most clinically available synthetic nerve grafts are only capable of facilitating neuroregeneration across small lesions (<5 mm). Review of electroconductive epolymers, hydrogel and composite systems confirmed carbon nano-tube (CNT) and polycaprolactone biomaterials as being suitable candidates for reparative nerve conduits or scaffolds. An electrospun microfiber fMWCNT-PCL composite conduit design was developed to re-connect large nerve gaps (>5 mm). Nested single-lumen and multi-lumen configurations with an insulating outer-portion were developed to mimic the fascicular architecture observed in peripheral nerves. Polymer solutions and composite suspensions were electrospun into microfiber membranes under the influence of 5 kV electric field. 80mm length conduit graft specimens were fabricated. Specimens were tension tested and found to have a Young's Modulus of 15.7 ± 2.9 MPa and a tensile strength of 1.17 ± 0.16 MPa and 1.37 ± 0.08 MPa for the single and multi-channel grafts respectively. Graft specimens were verified for spinal cord (kangaroo tail) attachment by suturing and did not result in tearing under 1.2 N tensile load. A preliminary neurotoxicity study using N2A cell-line confirmed cell-scaffold adhesion and viability.

Keywords: Peripheral nerve regeneration; Nerve repair; Grafting; Nerve guide conduit; Electrospinning; Neuroengineering; Poly(caprolactone); Carbon nanotubes; Multi-channel nerve guide

Introduction

Peripheral nerve injuries (PNI) and spinal cord injuries (SCI) are sustained by many each year. The nervous system is damaged by traumatic injury, surgery, cumulative trauma disorder, tumour, and is prevalent among aging populations. In the United States, 360,000 cases are reported for upper extremity paralytic syndromes on an annual basis, while more than 300,000 cases of peripheral nerve injuries occur in Europe annually [1]. Traumatic injuries occur due to compression, crush, stretch and laceration of the nervous tissue, resulting from an injury such as a motor incident, sporting injury, or traumatic fall. Trauma accounts for about 87% of all peripheral nerve injuries, while surgery accounts for roughly 12% (often as a result of tumour resection). Peripheral nerve injuries occur with surprisingly high frequency, reported in as many as 5% of all trauma patients [2].

Damage to the peripheral nervous system or spinal cord has severe consequences, including paralysis or major loss of sensory/motor function, as well as the stress on the mental health and financial situation of the patient and family. Less than 1% of people with an SCI fully recover, and the lifetime cost of a quadriplegic is estimated at greater than $1 million [3]. PNI is often less severe, but in many cases can result in significant loss of function or neuropathic pain, and depending on the severity may require extensive surgery. Autograft surgery is hardly an ideal treatment, due to nerve misalignment, loss of function at the donor site, and increased risk of infection. Furthermore, despite modern surgical techniques and equipment, functional restoration of the lesion is often inadequate, usually only 50% of cases exhibit good restoration of function [4].

At the present time, clinically available nerve grafts each have fundamental limitations, and usually produce substandard results when compared to autografts. Hence, they are typically used in a clinical setting only if the patient cannot undergo autograft surgery [5]. Detail on the mechanisms behind nervous system repair for the spinal cord [6] and peripheral nerves [7] are well known.

There is need to develop safe and efficacious grafting strategies to improve the function of patients suffering debilitating neural injuries. Recent approaches employ minimally invasive methods to deliver biocompatible and bioresorbable materials as scaffolds for tissue adhesion and growth, as well as for vehicles of molecules and stem cells that stimulate neuron growth and communication. This recent development in neuroengineering offers a promising alternative to conventional treatments, which removes the sacrifice of a healthy nerve (in cases of autograft surgery) and supports and guides the axons during their growth, while avoiding blood clot and scar tissue infiltration into the site of injury.

Electroconductive scaffolds have recently been considered. The use of electric current to stimulate neural cell differentiation, proliferation, adhesion and neural networking has the potential to facilitate nerve regeneration at an exceptional rate. Direct-current electric fields are present in all developing and regenerating animal tissues. It has been shown that endogenous electric fields (EF's) are present at the neurogenesis stages of embryonic development [8], and are involved with setting up a 3D structure of the nervous system [9]. However, their existence and potential impact on tissue repair and development are largely ignored [10].

Electrospun nanofibrous scaffolds have recently received much attention in tissue engineering due to the resemblance with collagen

***Corresponding author:** Philip Boughton, Biomedical Engineering, AMME School, The University of Sydney, Sydney, Australia, E-mail: philip.boughton@sydney.edu.au

Received June 03, 2013; **Accepted** July 14, 2013; **Published** July 20, 2013

Citation: Menzies CH, Lauto A, Mirto L, Gogh BV, Ruys A, et al. (2013) A Nested-Lumen Nerve Graft Design for Neuroengineering. J Biomim Biomater Tissue Eng 18: 105. doi: 10.4172/1662-100X.1000105

fibres in extracellular matrix, high surface area to volume ratio, their highly porous yet membranous structure, and the ability to be manipulated in terms of mechanical and degradable properties [11]. Poly (caprolactone) and carbon nanotubes were electrospun and used in this research for their micro scale architecture, in a conductive polymer composite.

Conductive polymer composites (CPCs) are a blend composed of a polymer matrix and electrical conductive fillers. PCL was chosen to be used as well-established biomaterial and relative to many other materials has been shown to facilitate more infiltration of neural tissue in growth, higher rate of myelination of fibres, and less infiltration of molecules and cells linked to inflammation [12]. PCL has also been shown to have moderated degradation rates that can match the rate of nerve regeneration. It is readily formed into nano wires using electro-spinning methods without adverse chemical change [13]. PCL is a component of an FDA-approved clinical nerve guide, 'Neurolac', hence its peripheral nerve regenerative capacity is well documented [14].

Carbon nanotubes (CNTs) are established as an electroconductive filler. They possess excellent electrical conductivity, excellent mechanical properties, and similar nanoscale features to neurites. Peer-reviewed studies report CNTs are not neurotoxic, can be modified to improve their neurite growth ability [15], have enhanced Neural Stem cell (NSC) differentiation and excitation *in vitro* [16]. They have also shown no toxicity to mice injected with multi-walled cabon nanotubes (MWCNTs) *in vivo* [17], and can be modified such that they are entirely cleared from the body of a mouse within 3hrs [18].

Zeng et al. showed that PCL maintains its well defined biodegradability profile when mixed with CNTs, meaning the PCL/CNT composite is feasible in this regard [19]. COOH functionalized MWCNTs were chosen because they have shown significantly lower cell production levels of IL-6 (an inflammatory cytokine) production when compared to pristine-MWCNTs and other functionalized variants (egOH-MWCNTs) [20], and have the best effect on cell biocompatibility, proliferation, or differentiation when compared to OH-MWCNTs, single-walled CNT (SWCNTs), and MWCNTs [21].

Standard safety procedures and guidance on material safety data sheets are important to follow as CNTs remain as a respiratory hazard and skin irritant [22]. To mitigate handling risks CNTs can be wetted and entrapped within polymer solution. Agglomeration even subsequent to mixing can result and may be approximated as spherical particles in a Newtonian fluid [23]. Ultrasound is commonly used to assist with minimizing agglomeration [20,24-26], and is probably the most widely used and effective mechanical technique for dispersing CNTs [27]. Electrospinning has been used to form CNT-polymer composite fibres and membranes [28]. Due to the high elongation of the polymer jet during electrospinning, the CNTs can orient along the fibre axis and are embedded in the fibre core [29].

Materials and Methods

Materials

The PCL utilized was of a high molecular weight linear polyester derived from caprolactone monomer, having a molecular weight of 80 000 GPC (Capa® 6800), purchased from Perstorp UK Ltd.

The CNTs were purchased from Cheap Tubes Inc. The COOH-MWCNTs were <8 nm in diameter, and 10-30 μm in length and for the rest of this report will be referred to as functionalised-MWCNTs, or 'f-MWCNTs'.

Methods

Conductive polymer composite production: The CPC was created firstly by creating a PCL solution in a 2L jar. It came in 3mm pellets and was stirred and heated (50°) with acetone to create the solution in the weight ratio of 1:4 (PCL: Acetone). Once the solution was consistent, f-MWCNTs were added.

The solution was formed so as to generate specimens with 20% wt. f-MWCNT (80% wt. PCL), and then diluted down into 10% and 5% wt. f-MWCNT composite. All 3 concentrations were sealed in separate containers so experiments could be performed on the different composites. The containers were maintained at 20% wt. composite with respect to the acetone vehicle.

Microscopic analysis: Polymer solutions were deposited as droplets onto glass slides and viewed using a Leica DMRXE optical microscope. Digital image analysis with software 'Leica QWin Plus' allowed agglomerates of f-MWCNT to be examined.

Dispersion of f-MWCNTs: Initial microscopy of the composite showed agglomerated f-MWCNT in small clusters and bundles, which meant they didn't possess a fibrous morphology in the composite solid. This is a significant problem because the fundamental properties that are trying to be incorporated into the composite (i.e.: high electrical conductivity and strong mechanical properties), become severely reduced. To counteract this, f-MWNT must be individually arranged in an electrically conductive network within the composite, and hence released from the agglomerates whilst in solution. In order to achieve this, shear force must be applied to the agglomerates within the liquid phase vehicle. In order to supply this force, 3 methods were tried:

Stirring/heating: firstly by hand vigorously using a stirring rod, and secondly by magnetic stirrer built into the hotplate, used at a rotation of ~50 rpm for 12 hours, at 60˚.

Ultrasonication: Ultrasonication is the action of applying ultrasound energy to a sample to cause agitation in particles, and was employed in this case to break up agglomerated f-MWCNTs. The ultrasound was supplied by a Vibra cell 501 model, at 20 kHz and 500 W (Sonics & Materials Inc.), for 3 s on, 1s off, total duration 40 mins. The ultrasound was delivered to the solution via a titanium tipped probe of 10 mm diameter.

Electrospinning equipment: Electrospun non-woven materials with high overall porosity, high surface area, flexibility and tensile support allow them to be suited to a wide variety of biomedical applications. Scaffold applications in tissue engineering have been a major focus of research activity. A Van de Graaff generator was coupled to Terumo needle connected to a 10 mL syringe filled with polymer solution or composite suspension. An earthed rotating aluminium cylinder was used as a collector and the whole assembly was shielded within a polycarbonate container. The voltage generated was sent through a high quality, thick gauge copper wire to the syringe tip. The needle used was a 20 gauge (0.9 mm outer diameter, 0.6 mm inner diameter) for the initial PCL electrospinning, and afterwards a copper tube (2 mm outer diameter, 1.1 mm inner diameter) replaced the needle for electrospinning of the composite.

Electrospinning of PCL solution: The electrospinning of PCL solution was initially tried to quickly calibrate and optimise the machine for use with the composite material; however it took multiple trials before this was achieved. It was initially set up so the syringe was filled with PCL 20% wt solution. After turning on the Van de Graaff

generator, the polymer solution and composite suspension were delivered at a rate of 250 μL/min. Electrospinning was conducted at standard lab conditions. The needle tip was adjusted to 180 mm from the collecting drum (which rotated at 5 revolutions per minute). A voltage of up to 5 kV was generated across this gap by the Van de Graaff generator.

Electrospinning of f-MWCNT/PCL Composite: The process used for electrospinning PCL was adjusted for the composite membrane formation. A closer spinning distance of 80 mm from needle to the collector was used. Other experimental parameters had to be modified as explained in the results/discussion with more detail.

Electrical conductivity testing: The three composites (5,10, and 20% wt. f-MWCNT) were all tested for electrical conductivity using a multimeter (Digital Multimeter QM1502 Cat II 250V) with a range of resistance from 20Ω to 2MΩ, similar to methods used in other studies [30].

The conductivity of the composite was then calculated using the following formula:

$$\sigma = l/(R \cdot A)$$

σ - Material conductivity in Siemens per meter (S/m - or more commonly S/cm for this application). R - resistance in Ohms, A - cross sectional area, and *l* - distance between the 2 aluminium plates.

Graft configuration: A conductive microfibre nested-lumen graft design with an insulating semi-permeable outer sheath was proposed as shown in figure 1.

Design specification requirements identified:

Nerve biocompatibility

Suture and adhesive compatible

Semi-conductive core, insulative sheath

Semi-permeable conduit sheath

Key-hole surgery compatible

Stability exceeding biologicals (12 wks)

Soft yet supportive

Good tensile strength

Avoid buckling instability

Resist buckling under compression

> 2 year shelf life

Fabrication process up-scalable and reliabile

Sterilizable

Single lumen and multi-channel lumen configurations were fabricated. The latter design involved nesting 4 smaller lumens within an external insulating layer. Multiple lumens may provide additional support against buckling and scaffolding for stabilizing tissue modelling and facilitating axonal growth cone progression.

6-8 mm diameter prototypes were formed using electrospun microfiber membrane. The configuration employed a novel concept with an outer insulating multi-layered fibrous conduit and nested electroconductive fibrous conduits. Report of this type structure has not been found in the review of the field of neuroengineering.

Tesile testing of the scaffolds: Tensile properties of the 2 different scaffold types were investigated using a Bose SP-AT with a 250 N load cell. Three scaffolds of each type were bonded at each end between 2 small pieces of cardboard (20 mm×30 mm) using cyanoacrylate before clamping. The dimensions of each sample were then measured using digital vernier callipers (IP54 150 mm Digital Caliper). The samples were tested to failure under tension, at a biomechanically relevant rate of 1 mm/sec. Bose Wintest 4 software was utilized to analyse data.

Surgical suture test: A kangaroo tail was dissected to allow access to the spine. A subsection of 10 cm was isolated containing 2 vertebrae, and then further stripped to reveal the spinal cord with care. The spinal cord was then sutured to one end of a scaffold sample (as per Figure 1) to simulate a surgical procedure, and loaded purely in tension to test its suturability and resistance to tear.

Neurotoxicity and cell adhesion assays: In this study, the neurotoxicity of electrospun nanofibref-MWCNT membranes were assessed for viability usingeuro-2A (N2A) cell line. The N2A cells are derived from mouse neuroblastoma cells and are widely used to study neuronal differentiation, neurite growth, synaptogenesis and signalling pathways [31]. Additionally, the ability of the scaffold morphology to accommodate cell adhesion was also determined. The N2A cells were cultured in functional Dulbecco's Modified Eagle's Medium (DMEM), with high glucose, 10% fetal calf serum, penicillin-streptomycin, and L-glutamate, and kept in an incubator for the duration of the experiment at 37˚ and 5% CO_2. Nanofibre samples were cut into 1 cm×1 cm squares, and then placed in a heat sealed semi-permeable packet, then treated with 70% ethanol.

The f-MWCNT and PCL samples were prepared in triplicates and adheared using a PCL / acetone adhesive in a 24 well plate. The controls were also prepared in triplicate and consisted of a control wells with untreated N2A and an adhesive control well with PCL adhesive coating the bottom of the well. Functional DMEM was used to rinse each specimen within the wells. Samples/controls were seeded with the N2A cells at a cell density of 16.9×10^4, and incubated for 24 hours at 5% CO_2, 37°C.

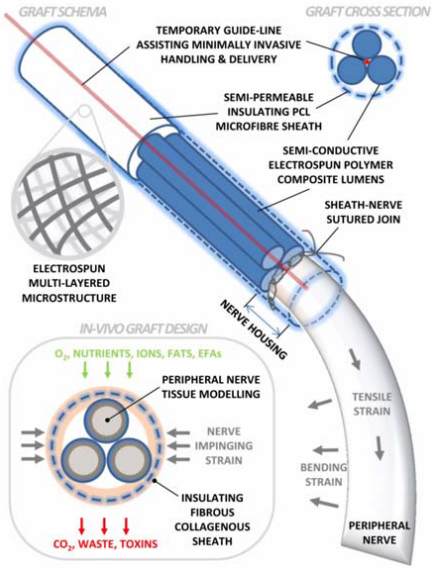

Figure 1: Biomimetic nested lumen nerve graft design.

After the 24 hour incubation, 10 µL of the supernatant (media) from each well was collected, and stained with trypan blue in the ratio 1:1. Using a haemocytometer, cells are counted according to whether they are stained by the trypan blue, allowing the ratio of viable: non-viable cells in the supernatant to be calculated. This assay was used to determine the adhering potential of the N2A cells to the f-MWCNT nanofibers as, a large number of viable cells which had not adhered meant that the cells poorly adhered to the microfibers.

To determine the neurotoxicity of the microfibers the in-well contents were collected. This was achived by dislodging the bound cells in each well with 500 µL of 0.1% trypsin with 5 minute incubation at 5% CO_2, 37°C. After the incubation period 2 mL of functional DMEM was added to each well to ensure the trypsin was diluted out and would not compromise the viability of the cells during the next haemocytometer counting stage. 10 µL of each cell suspension was stained with equal volumes of trypan blue and viable / non viable cells were counted using a haemocytometer. The data collected from both counts were used to calculate cell viability of each sample to give an indication of neurotoxicity.

Results and Discussion

Dispersion of CNT agglomerates

All methods of dispersing agglomerated f-MWCNT proved incomplete. This is a problematic for the successful formation of conductive scaffolds (as described before). f-MWCNTs could form fibrous interconnectivity network morphologies if separated, and accordingly, the fundamental characteristics and purpose of their incorporation (excellent electrical conductivity, strong mechanical properties, and nanoscale dimensions similar to neurites). Figure 2 displays 4 microscope shots (all at 200x) taken at various points in the composite's production. They show the small agglomerates of f-MWCNT, and the unsuccessful results after multiple attempts at dispersion. A comparison between the pictures allows firstly an understanding of what exactly is meant by 'agglomerate' in the material, and secondly an appreciation of the difficulty in breaking them apart.

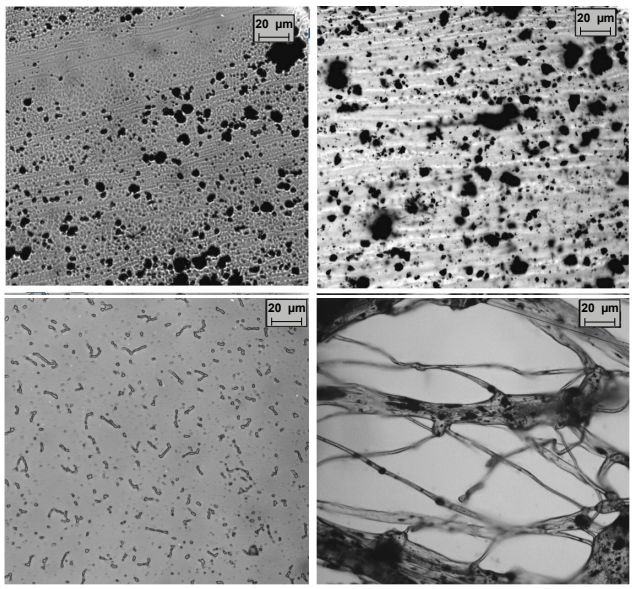

Figure 2: Micrographs (200x optical) of the composite material after different attempts to break up the agglomerates. Upper left: Taken immediately after mixing solution. Upper right: taken after ultrasonication. Bottom left: after pure acetone was squirted onto the microscope slide. Bottom right: After electrospinning.

The 'agglomeration' is caused by strong inter-molecular forces that originate from entanglements, electrostatic attraction, and high van der Waals forces of the f-MWCNTs [23]. Due to the nature of van de Waals forces, they are dependent on the distance between 2 particles, becoming much more intense when closer. This has a very important implication: once the initial f-MWCNT agglomerates have formed, they become very difficult to separate because the forces are harder to overcome at shorter distances. For the dispersion method, the external forces have to be strong enough to break or disrupt the agglomerates. As seen, the stress requirement needed to separate agglomerations of the nano-particles was not met through the variety of methods and electrospinning method [32]. Optimizing dispersion methods may enhance conductivity further.

The image corresponding to Figure 2: bottom left was taken after 1 mL of 100% acetone was deposited onto the microscope slide, and covered with a cover slip. f-MWCNTs were found to evenly disperse – something that was not evident with viscous PCL-acetone solution. The large addition of acetone lowered the viscosity significantly, hence lowering the shear needed to disperse the agglomerates. Accordingly, the even dispersion of the f-MWCNTs seen here presented a good representation of what the composite should look like after a successful dispersion. The diameters of the structures resolved are ≈1 µm, while the diameters of individual fibres are <8 nm, thus it is likely that in the most singular state, the f-MWCNTs form coil-like structures via intra-molecular forces.

Interestingly, after this solution was left to dry, the solution re-agglomerated. This secondary agglomeration must have formed immediately after the viscosity of the fluid reached an innate critical value, and has also been observed by others [33]. This observation is important because it draws the conclusion that using dispersion techniques for an extended amount of time, or at an increased intensity may not inhibit the formation of secondary agglomerates to the point of complete dispersion. This is an important factor to consider while preparing CNT nanocomposites. It also supports the concept of an 'inherent agglomeration factor' that can differ significantly based on the specific characteristics of the CNTs themselves, such as a functional group addition.

It has been previously shown that COOH modified CNTs do not

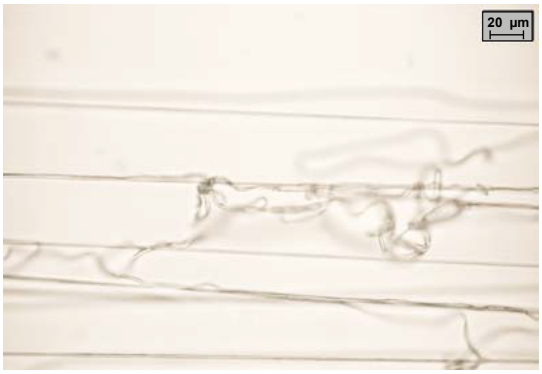

Figure 3: Microscopic image of PCL electrospun fibres approximately 1µm in diameter, verifying the relative uniformity of fibre produced using this method.

show even dispersion readily [34], supporting the findings in this work. For future studies, functionalised CNTs could be investigated for relative dispersion efficiencies.

Electrospinning

The initial tests involving PCL solution were consistent in forming good quality membranes on the aluminium collector. The electric field generated by the Van de Graaff generator was sufficient in producing the Taylor cone, and attracted the microfibres to the rotating drum effectively. After some configuration, the optimum specifics were found to be 23 cm above the aluminium drum collector, and 5 rpm, allowing the yield to easily peel off the spool.

Microscope analysis confirmed fibres were of consistent morphology (see Figure 3) comparable to other studies [35]; Greater than 90% of the fibres were ranging from 1-3 μm in diameter, concluding that this method was viable.

After the supposed optimisation of the electrospinning machine, microfibre mats were attempted to be created from the composite solution. This proved much more difficult than initially anticipated after the rapid success of the pure PCL electrospinning. Upon the initial trial using the 20 gauge needle (inner diameter = 0.6 mm) with 20% wt f-MWCNT, it became instantly clogged; preventing any electrospinning from happening. Similarly results were found when tested with 10% and 5% wt. solutions. To solve the problem, the needle was replaced with a 1.1 mm inner diameter copper tube.

The new inner diameter allowed the solution to run through it easily enough, but the small droplet did not make a fully formed Taylor cone. Instead, small, thick droplets (0.5–1 mm in size) built up and when heavy enough could drop from the surface and land on the collector (seen in Figure 2 - left). They had a 'beaded' formation with some resemblance to a fibre at one end. When a small amount of acetone was added to slightly dilute the solution, the surface tension was not great enough to hold the solution at the end of the needle tip, causing spinning flow to become unstable and separate into droplets.

Eventually, after much trial and error, it was found that 5% wt. f-MWCNT composite solution was the maximum possible for the given electrospinning setup. Sensitivity to suspension viscosity was apparent. The 10% and 20% solutions were not able to be electrospun using this apparatus, even subsequent to exhaustively varying parameters. The space between the copper tube and the collecting drum was decreased to just 5 cm, to allow an increase in electric field focus. This was a crucial factor that facilitate 5% composite to form a proper Taylor cone and hence, electrospin fibres.

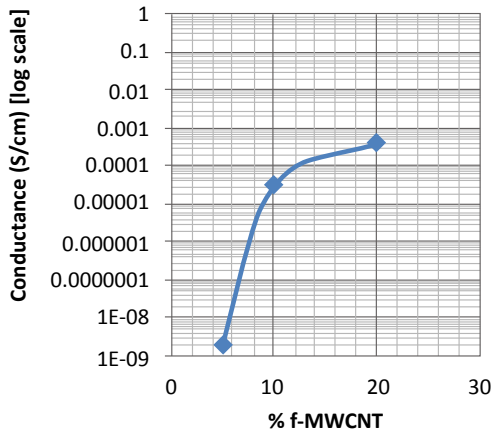

Figure 4: Conductivity of the composite at various f-MWCNT wt. %. Plot uses logarithmic values on the y axis to demonstrate percolation effect.

Electrical conductivity

The material conducted measurable amounts of electricity at the 10%, and 20% f-MWCNT concentrations, but not at 5%. This was most likely a result of the agglomeration of the f-MWCNT particles, as explained earlier. The material reached percolation at some point between 5%-10% wt. This posed a challenge may be addressed by improving CNT dispersion in PCL solution. The viable electrospun microfibre membrane with f-MWCNT was not able to conduct amounts of electricity measurable using a multimeter although may approach values that might still be beneficial for nerve cell guidance. 10% and 20% wt. batches were able to conduct measurable amounts of electricity (see Figure 4 for values).

Because the conductivity of the composite has a substantial descent somewhere between 5 and 10%, it is evident that electroconductivity breaks down somewhere between these values.

This can be explained by percolation theory, whereby at lower concentrations, the f-MWCNTs are rarely touching each other, and therefore cannot form conductive pathways through the material, due to the majority of the composite being insulating PCL matrix. Once a certain value of concentration is met, there are enough f-MWCNTs in the composite for electrons to follow certain conducting paths in the matrix, and percolation occurs, leading to a sudden rise in conductivity. The values of conductivity found in the experiment are notably in the semiconductor range of 10^{-8}–10^{3} S/cm [36].

Neurotoxicity study

In order to evaluate the ability of the two types of electrospun microfibre film's ability to facilitate growth and adhesion of neurons, the Neuro-2A (N2A) cell line was cultured on electrospun samples of both f-MWCNT composite and PCL. The results obtained from the neurotoxicity experiments were highly encouraging, showing minimal neurotoxicity and strong binding of cells to the microfiber. Additionally, statistical interpretation of the collected data showed no significant difference between the controls and microfiber sample wells ($P = 0.8123$ for adhearing assay and $P = 0.9839$ for neurotoxicity assay) further supporting the findings that the microfibers synthesised and tested in this study were not neurotoxic and allowed cells to bind to them.

From these experiments we were able to show statistically that the cells were healthy in all controls (N2A and PCL adhesive) and sample wells (See Figure 5A), and were able to adhere to both electrospun materials (See Figure 5B). The supernatant adhesion analysis shown in Figure 4B involved counting of viable and non-viable cells found in the media. Cells naturally adhere to surfaces using adhesive proteins (ref). Generally, non viable cells are unable to sustain the adhesive proteins and therefore do not adhere to surfaces whilst, viable cells are able to sustain these proteins and adhere. To find healthy cells in the media supernatant would be a sign that the cells adhesive proteins were not able to bind efficiently to the electrospun materials. However, as seen in Figure 5B, no viable cells were found in the supernatant suggesting that the cells were able to adhere sufficiently to both electrospun materials.

Additionally statistical interpretation of the data through a 1 way ANOVA showed that there was no statistical significance between any of the tested samples ($P = 0.8123$) further supporting the discovery that

the N2A cells were able to adhere to the electrospun composite as well if not better than the controls.

The neurotoxicity assay conducted in this study (See Figure 6A) revealed that there was an acceptable number of viable cells in all wells (controls and samples). A high cell viability is usually considered as >90% [37], meaning the cells were able to grow and proliferate readily in the environment. Comparing the f-MWCNT (98%) to the PCL (93%), we have shown that both microfibers are not neurotoxic and despite the data suggesting the cells grow better on the f-MWCNT microfiber this difference is not statistically relevant. Additionally, supporting the claim that the microfibers tested in this assay are not neurotoxic. We have shown there is no statistically significant difference between the control cells and the microfiber samples (P=0.9839).

Figure 6 shows microscopic images taken of the 2 electrospun materials, and the controls, and visualizes information mentioned in the above study. In Figure 6, the red outline highlights the large porous structures created by the electrospun microfibres of f-MWCNT composite. Evidently, the N2A cells preferentially bound in these pores as, can be seen by the distinct clumping of cells within these pores in Figures 6A and 6B. The electrospun PCL however, does not display the same result. As seen Figure 6D, the cells are significantly lower in numbers, and have not shown the same adhesion to that of the f-MWCNT composite, this reflects the difference in % viable cells shown in Figure 5A. This indicates that the electrospun f-MWCNT composite had no neurotoxic effects, and significantly increases the adhesion and viability of cells.

This biological study has verified the biocompatibility criterion regarding a major aspect of the peripheral nerve's local environment, and shown cells adhering deep within the interconnected pores throughout the sample. This is a significantly encouraging outcome in terms of this novel design of the nerve scaffold (mention how its no neurotoxic again perhaps or it might be to repedative).

Nested-Lumen graft prototype configuration

The prototypes featured 2 variations on scaffolds for use in neuroengineering, single lumen and multi-lumen variants. Both designs incorporated an inner layer comprised of f-MWCNT composite to allow electrical conductivity and enhance neuron regeneration, while the outer layer utilised pure PCL for its elastic and insulation properties.

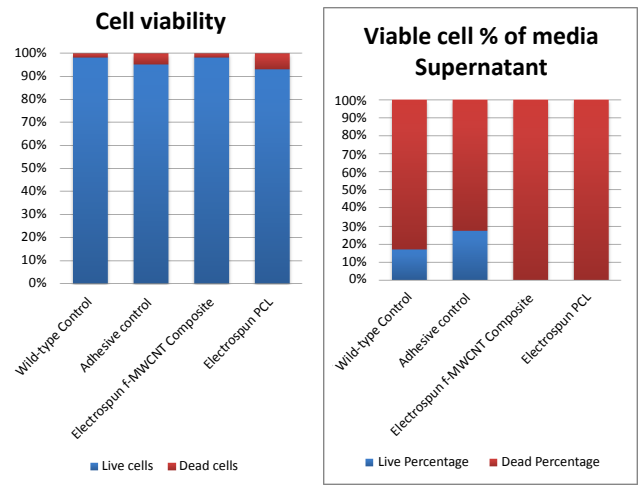

Figure 5: A. Cell viability results, B. Supernatent Adhesion analysis.

Inner conductive layer: The inner surface contained f-MWCNTs and was specifically tailored for the purpose of creating a niche surface for the neurite to grow and extend on. For further research this may involve the use of longitudinally aligned fibres. The electroconductive polymer surface was designed to enhance the recovery and extension of the neuron, improve the chances of re-innervating the neuron-specific target, as well as inducing the formation of complex neural networks [38].

The electroconductivity of the inner layer may also enable the use of an applied electrical current that runs from an electrode in one end to the other across the site of injury.

Outer insulating layer: The outer layer of the design is comprised of pure electrospun PCL, incorporated as the outer surface for a number of reasons:

Firstly, it is used simply to limit the amount of f-MWCNTs entering the body, as the long term effects of CNTs are not fully understood.

Functionally, the PCL layer was incorporated to the design because of its highly elastic nature when compared to the f-MWCNT composite. Hence it may help mitigate against collapse of the lumen hollow by counteracting any compressive force with an elastic restoration force.

The PCL should also act as an insulator for electrical activity in the internal conductive zone. This would not only act to restrict potentially harmful electric current leaking into the body when an external stimulus is applied, but would also enhance the effect of endogenously generated micro-currents by containing them to the localised site of neuroregeneration.

Single lumen scaffold: Single lumen nerve conduits are designed to influence axon growth to the distal stump, while preventing neuroma formation and infiltration of fibrous tissue. Single lumen devices are also thought to act as a distinct vessel, effective at localising Schwann cells and macrophages, and allowing trophic factors to accumulate. Generally, it maintains the injured site inside a chamber, acting as a separated environment from the rest of the body [39].

The scaffolds produced were relatively resilient and supportive,

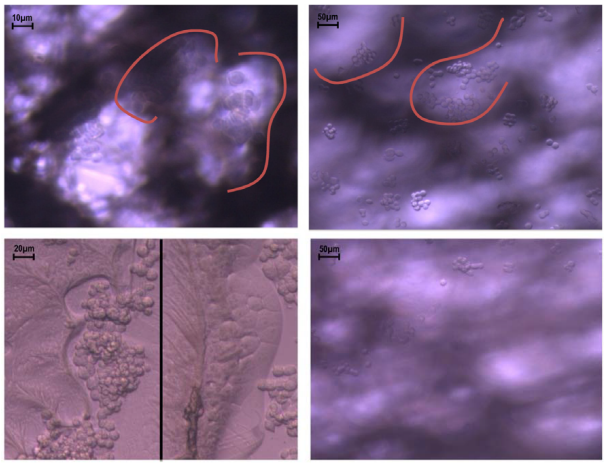

Figure 6: A,B Cell adhesion to the electrospun f-MWCNT, controls (C) and electrospun PCL (D. The control slide (C) is further divided into PCL adhesive control (left) and Wild-type (right), demonstrating wild type cell morphology was consistent in all samples, and N2A viability adjacent to PCL adhesive. Large porous structures are outlined in red, and show cells preferentially binding to them.

maintaining their shape adequately, while being compliant to a degree. When pinched between 2 fingers the scaffolds would restore to their original formation. When looking down into the lumen, it was clear that all lumens were fully expanded, and did not collapse after initial manufacture. The multi-lumen scaffolds were equally as robust.

Multi-lumen scaffold: The multi lumen scaffold is designed with 4 channels that run the length of the structure, but allowing for a nerve insertion zone. Several key reasons are behind the multi-lumen device:

The channels through the entirety of the graft serve as a biomimetic system of the multi-channel fascicular architecture and fibrous extracellular matrix found in native nerve. It is therefore designed to influence directed growth of neurons in a longitudinal manner.

Because they are created entirely with electrospun materials, the highly porous nature of the channels can facilitate transfer of important endogenous neurotrophins and neurotropins between each other.

Furthermore, the multi-lumen design may help mitigate against the risk of luminal collapse during surgical delivery or *in vivo* [40].

Tensile testing of scaffold prototypes: As expected, the two scaffold designs exhibited similar results. This was presumable a result of the individual lumens in the multi-channel device failing independently. While the test was being carried out, a definitive sound made it clear when each of the thin channels failed. In every sample, the f-MWCNT composite failed before the PCL. This was expected, as the f-MWCNT addition is known to increase strength, but decrease strain to failure.

Tensile strength: The average tensile strengths were similar but slightly higher in the multi-lumen design compared to the single lumen of 1.37 ± 0.08 MPa and 1.17 ± 0.16 MPa respectively. This is as expected as more electrospun f-MWCNT composite membrane was used to fabricate the multi-lumen samples. These values are slightly less than ideal, but are within the range of values obtained for peripheral nerves obtained in animal studies: ≈2-10 MPa [41,42].

Young's modulus: It was found that both configurations had similar loading profiles. The Young's Modulus of a typical nerve has been shown as 0.4-0.7 MPa in an animal model [41]. Both nerve grafts tested had an equivalent modulus of 15.70 ± 2.98 MPa. This is greater than values found in animal studies [41,42].

In practise, this means that the synthetic nerve graft will mechanically stabilize modelling nerve tissue through its structure, more than compared to a nerve. If either graft were implanted *in vivo*, physiological tension applied across the nerve would be shielded by the synthetic graft, possibly having a protective effect on the delicate nerve fibres in its centre that are undergoing regeneration where the axonal cones meet.

Porosity: The electrospinning machine produced ultra-thin fibre meshes that had a high surface area, and even high porosity with interconnected pores. The rough size of the pores could be measured using images taken during optical microscopy. It was found that the pore size had a large range in size, anywhere from 20-300 μm. Limitations of the electrospinning process played a significant role in this, specifically the insufficient control over the fibre diameter and the morphology of the film, usually causing non-uniform fibre meshes.

It is well understood that the porosity should approach a value sufficient for nutrient and gas exchange, retaining growth factors, and prevention of scarring. A value of 10–38 μm pore size has been proposed [43]. The lower limit should go no lower than 5-, as capillaries need to infiltrate and provide nutrients to the regenerating tissue. Likewise, it must not be too porous, as fibroblasts (possible responsible for scar tissue formation) can grow and proliferate in pores 15-100 μm [44]. Thus, an ideal size exists.

The maximum limit of pore sizes observed in material created using the electrospinning setup was extremely large, and most likely permissive to scarification, however, the high porosity facilitated the seeding and strong adhesion of N2A cells, validating the high surface area morphology caused by electrospinning. In the final design of the conduit, the process of rolling multiple layers tightly onto each other was devised as mitigation against this. *In vivo* tests should be performed to evaluate the configuration further.

Surgical suture test: The suture test aimed to verify whether the graft could meet some basic surgical requirements. The setup is shown in Figure 7. Firstly, suturing of the scaffold to the spinal cord showed that the scaffold could be sutured to a damaged nerve with relative ease, and maintains structural integrity when used for its intended purpose. Secondly, a weight of 1.2 N was hung from the bottom of the scaffold to prove that the sutures and scaffold would remain stable under some tensile load similar to what one might find during manipulation in an actual surgery.

Conclusion

Nested-lumen nerve graft prototypes were reliably fabricated. The novel configuration provides an insulating layer around conductive composite lumens. Preliminary surgical, tensile and neurotoxic responses were determined and found to be within acceptable ranges. If the CNT-polymer dispersion process could be improved, this nested-lumen graft design is likely to find *in vitro*-analytical and *in vivo*-clinical relevance.

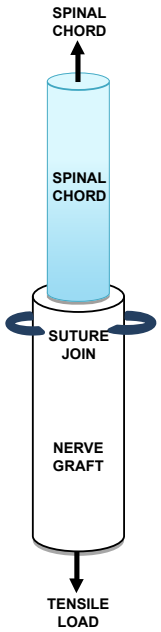

Figure 7: Surgical suture test.

References

1. Chiono V, Tonda-Turo C, Ciardelli G (2009) Chapter 9: Artificial scaffolds for peripheral nerve reconstruction. Int Rev Neurobiol 87: 173-198.
2. Brushart TME (1991) The Mechanical & Humoral Control of Specificity In Nerve Repair. Operative Nerve Repair and Reconstruction.
3. Girardi FP, Khan SN, Cammisa FP Jr, Blanck TJ (2000) Advances and strategies for spinal cord regeneration. Orthop Clin North Am 31: 465-472.
4. Pfister BJ, Gordon T, Loverde JR, Kochar AS, Mackinnon SE, et al. (2011) Biomedical engineering strategies for peripheral nerve repair: surgical applications, state of the art, and future challenges. Crit Rev Biomed Eng 39: 81-124.
5. Kehoe S, Zhang XF, Boyd D (2012) FDA approved guidance conduits and wraps for peripheral nerve injury: a review of materials and efficacy. Injury 43: 553-572.
6. Yiu G, He Z (2006) Glial inhibition of CNS axon regeneration. Nat Rev Neurosci 7: 617-627.
7. Deumens R, Bozkurt A, Meek MF, Marcus MA, Joosten EA, et al. (2010) Repairing injured peripheral nerves: Bridging the gap. Prog Neurobiol 92: 245-276.
8. Hotary KB, Robinson KR (1992) Evidence of a role for endogenous electrical fields in chick embryo development. Development 114: 985-996.
9. Shi R, Borgens RB (1995) Three-dimensional gradients of voltage during development of the nervous system as invisible coordinates for the establishment of embryonic pattern. Dev Dyn 202: 101-114.
10. Huang YC, Huang YY (2006) Biomaterials and strategies for nerve regeneration. Artif Organs 30: 514-522.
11. Subramanian A, Krishnan UM, Sethuraman S (2011) Fabrication of uniaxially aligned 3D electrospun scaffolds for neural regeneration. Biomed Mater 6: 025004.
12. Wong DY, Leveque JC, Brumblay H, Krebsbach PH, Hollister SJ, et al. (2008) Macro-architectures in spinal cord scaffold implants influence regeneration. J Neurotrauma 25: 1027-1037.
13. BÃ¶lgen N, MenceloÄŸlu YZ, Acatay K, Vargel I, PiÅŸkin E (2005) *In vitro* and *in vivo* degradation of non-woven materials made of poly(epsilon-caprolactone) nanofibers prepared by electrospinning under different conditions. J Biomater Sci Polym Ed 16: 1537-1555.
14. Bertleff MJ, Meek MF, Nicolai JP (2005) A prospective clinical evaluation of biodegradable neurolac nerve guides for sensory nerve repair in the hand. J Hand Surg Am 30: 513-518.
15. Mattson MP, Haddon RC, Rao AM (2000) Molecular functionalization of carbon nanotubes and use as substrates for neuronal growth. J Mol Neurosci 14: 175-182.
16. Kam NW, Jan E, Kotov NA (2009) Electrical stimulation of neural stem cells mediated by humanized carbon nanotube composite made with extracellular matrix protein. Nano Lett 9: 273-278.
17. Schipper ML, Nakayama-Ratchford N, Davis CR, Kam NW, Chu P, et al. (2008) A pilot toxicology study of single-walled carbon nanotubes in a small sample of mice. Nat Nanotechnol 3: 216-221.
18. Singh R, Pantarotto D, Lacerda L, Pastorin G, Klumpp C, et al. (2006) Tissue biodistribution and blood clearance rates of intravenously administered carbon nanotube radiotracers. Proc Natl Acad Sci U S A 103: 3357-62.
19. Zeng HL, Gao C, Yan DY (2006) Poly(?-caprolactone)-Functionalized Carbon Nanotubes and Their Biodegradation Properties. Adv Funct Mater 16: 812-818.
20. Baktur R (2011) A study on the applications and toxicity assessments of carbon nanotubes in tissue engineering, in All Graduate Theses and Dissertations. Paper 928.2011, Utah State University: United States -- Utah. p. 100.
21. Mooney E, Dockery P, Greiser U, Murphy M, Barron V (2008) Carbon nanotubes and mesenchymal stem cells: biocompatibility, proliferation and differentiation. Nano Lett 8: 2137-2143.
22. Cheap-Tubes-Inc. (2009) Material Safety Data Sheet. Company Website.
23. Pegel, S, Potschke P, Petzold G, Alig I, Dudkin SM, et al. (2008) Dispersion, agglomeration, and network formation of multiwalled carbon nanotubes in polycarbonate melts. Polymer 49: 974-984.
24. Thurnherr T, Brandenberger C, Fischer K, Diener L, Manser P, et al. (2011) A comparison of acute and long-term effects of industrial multiwalled carbon nanotubes on human lung and immune cells *in vitro*. Toxicol Lett 200: 176-186.
25. Liu HL, Zhang YL, Yang N, Zhang YX, Liu XQ, et al. (2011) A functionalized single-walled carbon nanotube-induced autophagic cell death in human lung cells through Akt-TSC2-mTOR signaling. Cell Death Dis 2: e159.
26. Montes-Fonseca SL, Orrantia-Borunda E, Aguilar-Elguezabal A, González Horta C, Talamás-Rohana P, et al. (2012) Cytotoxicity of functionalized carbon nanotubes in J774A macrophages. Nanomedicine 8: 853-859.
27. Ruan B, Jacobi AM (2012) Ultrasonication effects on thermal and rheological properties of carbon nanotube suspensions. Nanoscale Res Lett 7: 127.
28. Salalha W, Dror Y, Khalfin RL, Cohen Y, Yarin AL, et al. (2004) Single-walled carbon nanotubes embedded in oriented polymeric nanofibers by electrospinning. Langmuir 20: 9852-9855.
29. Baji A, Mai YW, Wong SC, Abtahi M, Chen P (2010) Electrospinning of polymer nanofibers: Effects on oriented morphology, structures and tensile properties. Compos Sci Technol 70: 703-718.
30. Wang Q, Dai J, Li W, Wei Z, Jiang J (2008) The effects of CNT alignment on electrical conductivity and mechanical properties of SWNT/epoxy nanocomposites. Compos Sci Technol 68: 1644-1648.
31. Tremblay RG, Sikorska M, Sandhu JK, Lanthier P, Ribecco-Lutkiewicz M, et al. (2010) Differentiation of mouse Neuro 2A cells into dopamine neurons. J Neurosci Methods 186: 60-67.
32. Subbiah T, Bhat GS, Tock RW, Parameswaran S, Ramkumar SS (2005) Electrospinning of nanofibers. J Appl Polym Sci 96: 557-569.
33. Nadler M, Werner J, Mahrholz T, Riedel U, Hufenbach W, et al. (2009) Effect of CNT surface functionalisation on the mechanical properties of multi-walled carbon nanotube/epoxy-composites. Compos Part A Appl Sci Manuf 40: 932-937.
34. Zhao B, Wang J, Li Z, Liu P, Chen D, et al. (2008) Mechanical strength improvement of polypropylene threads modified by PVA/CNT composite coatings. Materials Letters 62: 4380-4382.
35. Rana S, Cho J (2011) Core-sheath polyurethane-carbon nanotube nanofibers prepared by electrospinning. Fibers and Polymers 12: 721-726.
36. Guimard NK, Gomez N, Schmidt CE (2007) Conducting polymers in biomedical engineering. Progress in Polymer Science 32: 876-921.
37. Wu Z, Hjort K, Wicher G, Fex Svenningsen A (2008) Microfluidic high viability neural cell separation using viscoelastically tuned hydrodynamic spreading. Biomed Microdevices 10: 631-638.
38. Bechara S, Wadman L, Popat KC (2011) Electroconductive polymeric nanowire templates facilitates *in vitro* C17.2 neural stem cell line adhesion, proliferation and differentiation. Acta Biomater 7: 2892-2901.
39. Belkas JS, Shoichet MS, Midha R (2004) Axonal guidance channels in peripheral nerve regeneration. Operative Techniques in Orthopaedics 14: 190-198.
40. Yao L, de Ruiter GC, Wang H, Knight AM, Spinner RJ, et al. (2010) Controlling dispersion of axonal regeneration using a multichannel collagen nerve conduit. Biomaterials 31: 5789-5797.
41. Borschel GH, Kia KF, Kuzon WM Jr, Dennis RG (2003) Mechanical properties of acellular peripheral nerve. J Surg Res 114: 133-139.
42. Rydevik BL, Kwan MK, Myers RR, Brown RA, Triggs KJ, et al. (1990) An *in vitro* mechanical and histological study of acute stretching on rabbit tibial nerve. J Orthop Res 8: 694-701.
43. Kokai LE, Lin YC, Oyster NM, Marra KG (2009) Diffusion of soluble factors through degradable polymer nerve guides: Controlling manufacturing parameters. Acta Biomater 5: 2540-2550.
44. Ma J, Wang H, He B, Chen J (2001) A preliminary *in vitro* study on the fabrication and tissue engineering applications of a novel chitosan bilayer material as a scaffold of human neofetal dermal fibroblasts. Biomaterials 22: 331-336.

Citation: Menzies CH, Lauto A, Mirto L, Gogh BV, Ruys A, et al. (2013) A Nested-Lumen Nerve Graft Design for Neuroengineering. J Biomim Biomater Tissue Eng 18: 105. doi: 10.4172/1662-100X.1000105